Enhanced Water Desalination by Increasing the Electroconductivity of Carbon Powders for High Performance Flow-electrode Capacitive Deionization

Kexin Tang,[a,b,c] Sotira Yiacoumi,[a] Yuping Li,[b] Costas Tsouris*[a,d]

[a] School of Civil and Environmental Engineering, Georgia Institute of Technology, Atlanta, Georgia 30332-0373, USA

[b] Institute of Process Engineering, Division of Environment Technology and Engineering, Beijing Engineering Research Center of Process Pollution Control, Chinese Academy of Sciences, Beijing 100190, PR China

[c] School of Chemical Engineering and Technology, National Engineering Research Center for Distillation Technology, Tianjin University, Tianjin 300072, PR China

[d] Oak Ridge National Laboratory, Oak Ridge, Tennessee 37831-6181, USA
*Email: tsourisc@ornl.gov; Telephone: 865-241-3246

Submitted for publication in

ACS Sustainable Chemistry & Engineering

September 2018

Revised: November 2018

Abstract

Flow-electrode capacitive deionization (FCDI) can be improved via enhanced charge transfer by increasing the flow-electrode (FE) conductivity. Since water is the main component of FE (>70%), the key to improving the electroconductivity lies in the properties of carbon materials. In this work, three types of carbon powders, i.e., activated carbon (AC); mesoporous carbon; and carbon nanotubes (CNTs), were employed in FEs to investigate the influence of powder properties on the FCDI performance. The morphology and structure of powders and electrochemical behavior and rheology of FEs were investigated to reveal the relationship between FE properties and desalination performance. Results show that, due to their unique electrosorption behavior, excellent conductivity, and enhanced conductivity through a bridging effect, CNTs based FE (carbon loading: 3 wt.%) achieved the fastest (8.3 mg s^{-1} m^{-2}) and the most stable desalination (charge efficiency: 93.3%). A faster desalination (13.2 mg s^{-1} m^{-2}), due to significantly improved electroconductivity (13.2 times) with only a slight viscosity increase (1.1 times), was achieved by adding CNTs into 6.91 wt.% AC-based FE for a 7.41 wt% total carbon concentration. This study highlights the importance of the intrinsic properties of carbon materials, especially electroconductivity, in promoting FCDI desalination performance.

Keywords: Flow-electrode capacitive deionization, carbon nanotubes, desalination, electrochemical impedance spectroscopy, charge/ion transfer

Note: A list of all abbreviations used in this manuscript appears in Table S8 of the supporting information

INTRODUCTION

Capacitive deionization (CDI) has been intensively investigated in the last decade for its potentially low energy demand and eco-friendly operation.[1] Due to the poor cycling performance and co-ion rejection effect, however, industrial applications of CDI have rarely been reported. Alternatively, membrane CDI (MCDI) utilizing ion exchange membranes attached to the surface of the electrodes can be used to achieve high and fast salt removal and limit co-ion rejection.[2-3] One example of an industrial application for CDI and MCDI is Voltea B.V. (CAPDI©, Netherlands). Even though MCDI can handle large-scale desalination through the development of new electrode materials,[4] design of new devices,[5-6] optimization of process operation,[7-8] and module stack-up,[9] the intermittent cyclic operation and solid-carbon-electrode sheets still need substantial improvements for expanded future applications. The electrodes in the CDI and MCDI processes are stationary and prepared and attached to current collectors via polymer binders. Such polymer binders as polytetrafluoroethylene may block a significant portion of the pores in carbon electrodes and introduce hydrophobic surfaces into the electrodes, ultimately reducing their salt adsorption performance.[10] Furthermore, when the electrodes are saturated with ions during operation, electrode regeneration is required, leading to intermittent operation.

Previous studies have indicated that flow-electrodes (FE; hereafter the MCDI process utilizing FE is termed FCDI) can be employed to solve issues caused by the stationary electrodes used in CDI and MCDI,[11-14] i.e., the intermittent operation and hydrophobic polymer binder in electrodes. Self-regeneration outside the FCDI module, without using binders, allows FE to theoretically provide infinite surface area for ion adsorption.[11] A typical FCDI module is symmetrically assembled from end plates, current collectors, FEs, ion exchange membranes (IEMs), and a salt water feed channel, where the FEs typically flow through engraved channels on the current

collectors' surface. As the main functional component of FCDI, a FE is generally composed of carbon powder and aqueous electrolyte.[15-16] The maximum reported carbon loading for FE is approximately 28 wt.%.[12] In this case, even if the electrolyte salt concentration is 0.5 M, the water content could still be approximately 70 wt.%. Thus, since water is its main component, a FE is not a very good electrical conductor.

Several strategies have been developed for enhancing FE conductivity including increasing the carbon loading[12] or electrolyte concentration,[17] utilizing FE as a fluidized bed,[13] using spherical carbon particles,[18] performing surface oxidation treatment of carbon particles,[18] and introducing additives such as carbon black[16] or redox couples.[19] Although these methods are reported to have improved the FCDI performance, they may also introduce additional problems; for example, increasing the carbon loading increases the FE viscosity,[20] introducing a risk of flow clogging. Also, by increasing the electrolyte concentration to levels higher than those of treated solutions, diffusion against the concentration gradient in FCDI will be reduced. Furthermore, surface modification of carbon powder may be an issue for long-term operational stability. Since the electrolyte concentration cannot be significantly increased, the key to enhancing FE conductivity lies in the inherent properties of carbon materials, e.g., good conductivity for charge transfer and the ability to maintain high frequency collisions between particles or particles and current collectors.

Carbon nanotubes (CNTs) are a possible candidate to meet all previously mentioned requirements. CNTs have unique tubular structure and electronic and mechanical properties.[21] They have been investigated for energy storage applications (batteries and supercapacitors),[22-23] photovoltaic conversion,[24] hydrogen adsorption and storage,[25] field emission,[26] sensors and probes,[27] etc. They are also widely used for electrode[28-29] or membrane[30] modification for

enhanced electrochemical and separations applications. CDI or MCDI electrodes made of CNTs, however, could not compete with those from other porous carbon materials due to the difficulty of uniformly dispersing CNTs in stationary electrodes[29, 31] and the need to use adhesive polymers. Moronshing et al.[32] recently developed a scalable CNT-thread electrode in which CNTs are bonded with cellulose fibers through van der Waals attraction to achieve fast CDI performance. One of the benefits of using well-dispersed nanotubes without adhesive polymer is that both the interior and exterior surfaces, as well as the spaces between nanotubes, are accessible to ions.[32] Notably, CNTs can be metallic or semiconducting depending on the diameter and chirality.[33] Therefore, metallic and well-dispersed CNTs may have excellent FCDI desalination performance as well.

Since electrodialysis (ED) or FCDI using carbon-free FEs is considered to contribute to FCDI desalination,[15] and the different properties (e.g., particle shape, pore structure, and conductivity) of carbon materials such as activated carbon (AC), mesoporous carbon (MC), and CNTs also impact the FCDI performance, the specific objectives of this work were to: (1) evaluate the FCDI performance using FE composed of metallic CNTs by comparing results with ED and other FCDI devices where conventional carbon materials such as AC and MC are used; (2) elucidate the importance of FE electroconductivity on high and fast salt removal, by using CNTs as FE additive at different dosage levels and examining the electrochemical characteristics of FEs; and (3) propose a possible charge/ion transfer pathway in the FEs containing CNTs, to provide guidance for subsequent development of FEs for more effective and energy efficient FCDI.

EXPERIMENTAL SECTION

Preparation of flow-electrodes. FEs were obtained by dispersing carbon powders in electrolyte solution (129 mL, 0.2 M NaCl) under continuous sonication (24 hours) and subsequent vigorous magnetic stirring (48 hours).[11, 15] For materials information please refer to Text S1 and Tables S1-

S2 of the supporting information. Two different carbon loadings were prepared for specific experimental purposes described below (Table S3):

(1) Evaluate the FCDI performance using different carbon materials. Since FEs composed of CNTs cannot flow when the carbon loading exceeds 3 wt.%, three types of FEs using AC (FE-AC), MC (FE-MC) and CNTs (FE-CNTs) with 3 wt.% carbon loading were prepared. In addition, for comparison, an ED experiment (carbon loading: 0.0 wt.%) was conducted under identical conditions.

(2) Use CNTs as FE-AC additives. Since FEs generally behave better at higher carbon loadings,[12-13] the carbon loading was further increased to 7.41 wt.% for FE-AC, where the CNT loading varied from 0.0 wt.%, to 0.5 wt.%, to 1.0 wt.%, which were correspondingly termed as FE-AC-T0, FE-AC-T0.5 and FE-AC-T1.0.

Setup and operation of FCDI experiments. The FCDI process diagram is shown in Figure S1. The FEs were pumped through serpentine shaped grooves (Figure S2A) on the surface of the graphite current collectors, where the contact area between FE and graphite plate or between FE and feed solution (FS) is 130.4 cm^2 or 43.2 cm^2, respectively. The FE suspension was simultaneously pumped from a common reservoir into the anode and cathode channels at a flow rate of 25 mL min^{-1} each, and then back to the reservoir, by a dual-head pump (Model 7518-00, Cole Parmer). The FE reservoir was constantly stirred to prevent settling and aggregation of carbon particles. Another peristaltic pump (Model RP-1, Dynamax) was used to deliver FS (0.2 M NaCl, 129 mL) into the FCDI unit at a flow rate of 10 mL min^{-1}. The FE and FS were in circulation during all of the experiments. An electrical potential (1.6 V) was provided to the FCDI system by a direct current (DC) power supply (HP, 3632A), and the current response of the FCDI device was continuously monitored. The applied potential of 1.6 V was adopted after a series of preliminary

experiments under various applied potentials (V = 1.2, 1.6, 2.0, and 2.4 V). In this preliminary work, the desalination performance increased with increasing potential but, due to Faradaic reactions, the average charge efficiency decreased significantly beyond 1.6 V. Thus, the optimum potential for the work presented in this paper was determined to be 1.6 V. A conductivity meter (Model 3082, Amber Science) was employed to continuously record the conductivity of FS. The pH values of FS and FE were measured every 30 minutes by a pH meter (Accumet pH meter 50, Thermo Scientific). The salt removal capacity (SRC, mg g^{-1}), salt removal rate (SRR, mg s^{-1} m^{-2}), charge efficiency (Λ) of FCDI desalination were obtained from eq. S1-S3 (Text S2).

Electrochemical impedance spectroscopy and Rheology measurements. To reduce the mass of carbon needed for the electrochemical impedance spectroscopy (EIS) measurements, we designed and fabricated a small-scale FCDI device of similar geometry (Figure S2B and Table S4). The depth and width of the grooves on the graphite plates are 2 and 3 mm, respectively, and the contact area between FE and graphite plate or FE and FS is 22.4 cm^2 or 9.2 cm^2, respectively. The volumes of FEs and FS were reduced to 50 mL each due to the smaller size of this device compared to the size of the one described in Section 2.2 and in the supporting information. Typically, EIS measurements of FEs in previous studies were conducted in a static cell.[17, 34-35] Here, to prevent particle settling and aggregation and to provide electrochemical information under realistic FCDI process conditions, we operated this small device under conditions identical to those used for the operation of the larger device mentioned in Section 2.2. The EIS testing method involved an alternating current signal of amplitude 10 mV and frequency varying from 10^5 to 0.01 Hz applied to the FCDI system through an Autolab electrochemical workstation (PGSTAT302N, Metrohm).

Rheology measurements for FEs were carried out using a torsional rheometer (MCR302, Anton Paar, Austria), where steady shear viscometry was performed and the shear rate decreased from 100 to 0.001 s^{-1}.

RESULTS AND DISCUSSIONS

Superior desalination performance of FE-CNTs. Morphology and structure characterization results indicate that carbons employed in this work have vastly different morphology and pore and graphite structure (Text S3-S4 and Table S5), and these properties may affect their electroconductivity and, consequently, their desalination performance. Therefore, FEs consisting of 3 wt.% AC, MC, or CNTs were employed for FCDI experiments. In addition, an ED experiment without carbon material was carried out to investigate its contribution to the FCDI desalination performance.

Figure 1 shows the time-dependent decrease in the NaCl concentration, *SRR* value, and charge efficiency for FCDI systems using ED, FE-MC, FE-AC and FE-CNTs. Among these FEs, the FE-CNTs enables the fastest and the most stable desalination performance. Specifically, as shown in Table S6, after 360 minutes, the *SRC* value of FE-CNTs (284.3 mg g^{-1}) was 4.1 and 19.7 times greater than that of FE-AC (69.7 mg g^{-1}) and FE-MC (14.4 mg g^{-1}), respectively. Although *SRC* in FCDI can increase as long as the system is running, this metric can provide information on the differences in the desalination capacities of these FEs over long periods of operation. The average desalination rates of ED, FE-MC, FE-AC, and FE-CNTs derived from Figure 1B were 0.47, 0.86, 2.78, and 8.32 mg s^{-1} m^{-2}, respectively, demonstrating a desalination rate of FE-CNTs 17.7, 9.7, and 3.0 times greater than those of ED, FE-MC, and FE-AC, respectively. Furthermore, the charge efficiency exhibited by FE-CNTs (93.3%) is much higher than the charge efficiency of ED (73.0%), FE-AC (73.5%), and FE-MC (67.8%) (Figure 1C).

These results suggest that the FCDI desalination performance can be greatly enhanced by utilizing metallically conductive CNTs. The superior desalination performance of FE-CNTs among other FEs may be attributed to its excellent conductivity and weak Faradaic reactions. CNTs are a single or multi-layer graphene wrapped in a tube with excellent conductivity (Figure S3), which determines its lower resistance (see further discussion about the electroconductivity of FEs in Section 3.3). Because of proton and hydroxyl ion transport, as well as Faradaic reactions,

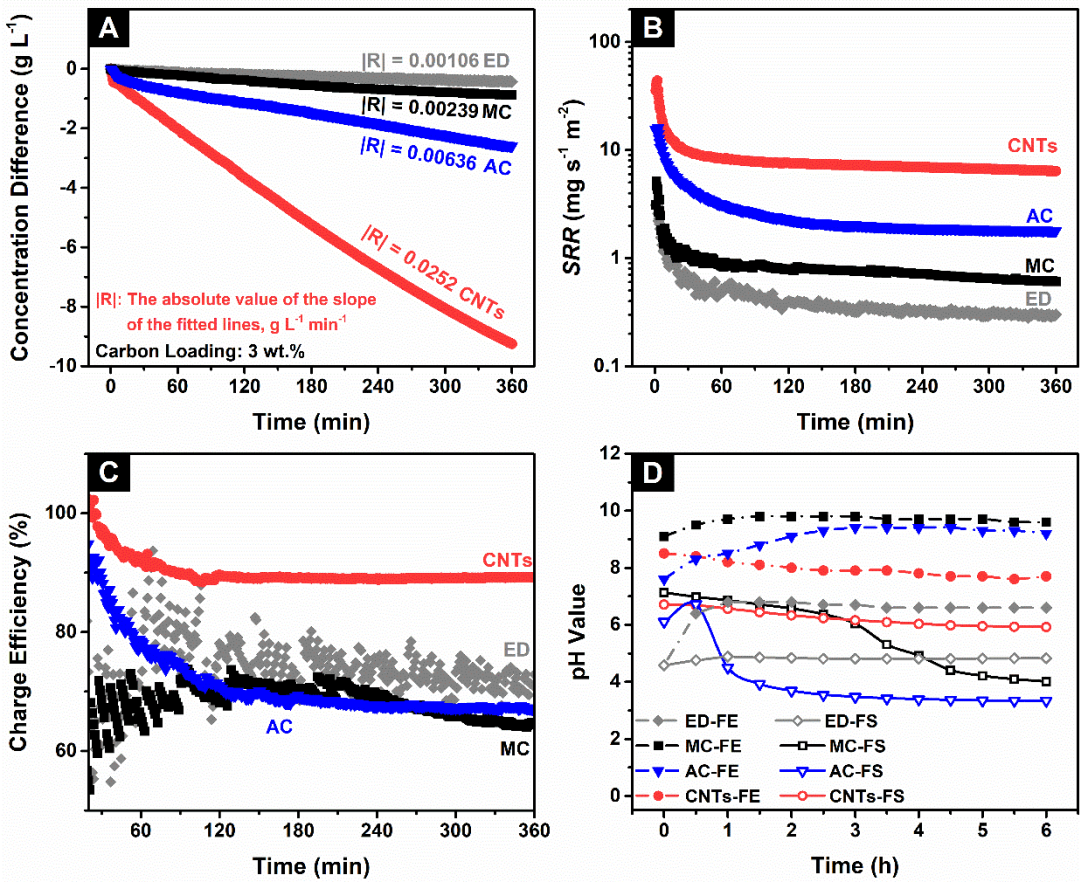

Figure 1 Time-dependent profiles for the FCDI system using different carbon powders as flow-electrodes: (A) concentration difference, (B) salt removal rate (*SRR*), (C) charge efficiency and (D) pH change of flow-electrode (FE) and feed solution (FS). The total carbon loading is kept at 3 wt.% for all FEs used.

the pH values in FE and FS during desalination diverged (Figure 1D). Due to the greater extent of Faradaic reactions,[15] the FE and FS of FE-AC and FE-MC became more alkaline and acidic, respectively, than those of the FE-CNTs.

In summary, the results presented in Figure 1 indicate that (i) the type of porous carbon material has profound influence on the FCDI desalination performance, and (ii) among the different types of carbon materials employed, CNTs are the most conducive medium for the charge/ion transport in FEs.

Using CNTs as Flow-electrode additive. Although FE-CNTs show excellent desalination performance, CNTs may not be a perfect candidate for practical FCDI applications as a result of its high market price and its low carbon loading. To utilize its superior FCDI desalination performance, however, we can employ CNTs as an FE additive for other low-cost, desalination-effective carbon materials, e.g. AC. Therefore, composite FEs were prepared including FE-AC-T0, FE-AC-T0.5, and FE-AC-T1.0 to investigate the effectiveness of CNTs as an additive for AC based FE.

According to the concentration differences graph in Figure 2A, after 360 minutes, the *SRC* values (Table S6) of FE-AC-T0, FE-AC-T0.5, and FE-AC-T1.0 were 121.7, 131.3, and 132.2 mg g^{-1}, respectively. Since the total amount of salt in FS was 1.509 g (0.2 M NaCl, 129 mL), the salt removal efficiencies reached 87.0%, 93.6% and 94.2% for FE-AC-T0, FE-AC-T0.5 and FE-AC-T1.0, respectively, even though the concentration difference between FE and FS could be as high as 20 g L^{-1}. Since the flow-electrodes were continuously recycled from the flow-electrode reservoir to the FCDI module (Figure S1), the results also indicate a stable cycling ability of the flow-electrodes. Moreover, the average desalination rate increased from 9.78 mg s^{-1} m^{-2} for FE-AC-T0 to 13.16 mg s^{-1} m^{-2} for FE-AC-T0.5 (Figure 2B). When the CNTs loading is increased from 0.5 to

1.0 wt.%, however, the desalination rates of FE-AC-T0.5 and FE-AC-T1.0 (12.86 mg s^{-1} m^{-2}) were similar. This phenomenon could be explained by any of the following reasons, which suggest that the addition of CNTs significantly increases FE conductivity, so that some other process step becomes the rate limiting mechanism:

(i) A limited amount of salt: As discussed above, FE-AC-T0.5 and FE-AC-T1.0 adsorbed nearly all ions from FS into FE, thus the performance difference between these two FEs becomes extremely small.

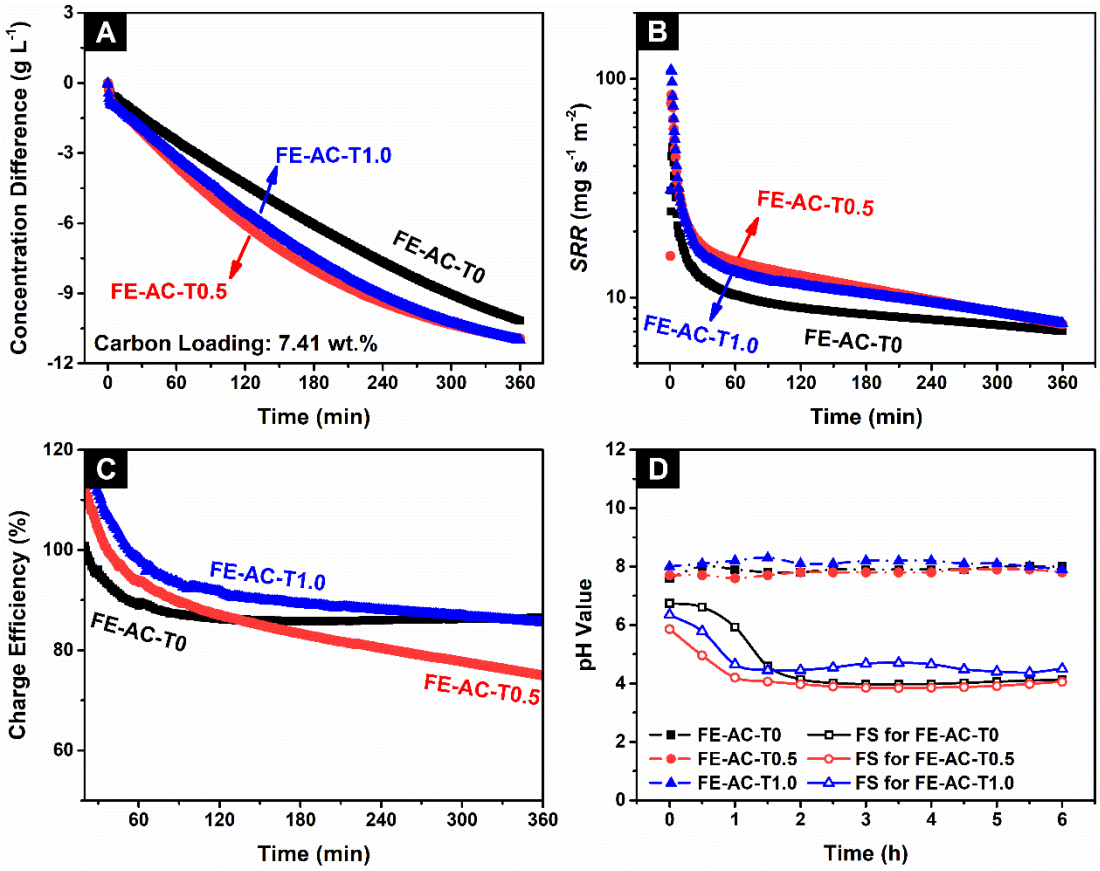

Figure 2 Time-dependent profiles for the FCDI system with CNTs as flow-electrode additive: (A) concentration difference, (B) salt removal rate (*SRR*), (C) charge efficiency, and (D) pH change of flow-electrode (FE) and feed solution (FS). The total carbon loading is 7.41 wt.% for all FE compositions.

(ii) Constantly changing driving force: As the desalination progressed, the concentration difference between FE and FS gradually increased, so that ion transport occurred against an increasing concentration driving force resistance. In combination with the low ion concentration in the desalinated solution, the increasing mass-transfer resistance leaves little room for improvement.

(iii) Changed FE rheology: Even though high-load CNTs are likely to enhance the electroconductivity of FE, increasing the CNTs content in FE also increases the viscosity of FE. The higher viscosity reduces the electrode fluidity, which is related to the electrode regeneration efficiency,[12] thus the charge/ion transport rate may be slowed down.

One advantage of increasing the CNTs loading to 1.0 wt.% is the enhancement in the charge efficiency (Figure 2C and Table S6). When the CNTs loading was 0.5 wt.%, the average charge efficiency was 89.8%, which is comparable to a pure AC electrode (89.9 %). In comparison, the average charge efficiency of FE-AC-T1.0 reached 97.9%. With time, however, the charge efficiencies of FE-AC-T0.5 and FE-AC-T1.0 gradually decreased, probably due to increasing transport resistance as discussed in the previous paragraph. When FE gains and FS loses ions, i.e., concentration polarization caused by the limited ions transport in the boundaries of IEMs,[36] FE is likely to decompose water. Thus, the charge efficiency decreases over time. Another impact of electrochemical reactions occurring in the FCDI system is pH fluctuation in FEs and FS. As summarized in Table S6, except for ED, the FEs and FS become basic and acidic, respectively. This phenomenon may be the result of a synergistic effect of multiple factors. First, proton and hydroxyl transport through the IEMs could produce pH changes in both FS and FE.[37] Second, as detected by Ma et al.,[38] since the generation of hydroxyl ions is easier than the generation of protons at 1.6 V,[16] the amounts of protons and hydroxyl ions generated in the anode and cathode

chambers is unbalanced, so that after charge neutralization, more hydroxyl ions remain in FEs. As the CNTs loading was increased, the pH of the FCDI system could still be maintained at a relatively stable level due to relatively high average charge efficiency.

The results of Table S6 indicate that, adding a certain amount of CNTs (e.g., 0.5 wt.%) in an AC based FE can effectively promote the desalination performance; however, excessive loading of CNTs not only cannot enhance desalination, but also wastes electrode materials and energy pumping a higher-viscosity fluid. Certainly, the influence of the CNTs loading on the desalination performance may vary with changing total carbon loading. For example, the influence of the viscosity can be reduced by decreasing the total carbon loading, while an increase in the CNTs loading may further enhance the FCDI performance. In practical applications, however, it is desirable to achieve rapid desalination, which can be accomplished by high carbon loading.[12, 20] Therefore, follow-up work should focus on finding inexpensive but highly effective carbon materials to promote FCDI desalination.

The influence of carbon powder types and CNTs addition on the FCDI performance suggests that the electroconductivity and rheology of FEs may synergistically affect the FCDI desalination performance. Thus, the electroconductivity (Section 3.3) and rheology (Section 3.4) of FEs under different FE compositions were specifically analyzed in the following two sections to investigate the mechanism of how charge/ion transfer is enhanced in CNTs-containing FEs (Section 3.4).

EIS analysis of the FCDI system. EIS was employed to analyze the electroconductivity of FEs. The charge/ion transfer in an FCDI process can be easily analyzed by considering FE as a homogeneous object rather than a mixture of electrolyte and carbon powder. The measured EIS plots were fitted using an equivalent circuit diagram to yield the values of the circuit components, which can be qualitatively associated to process transport parameters.

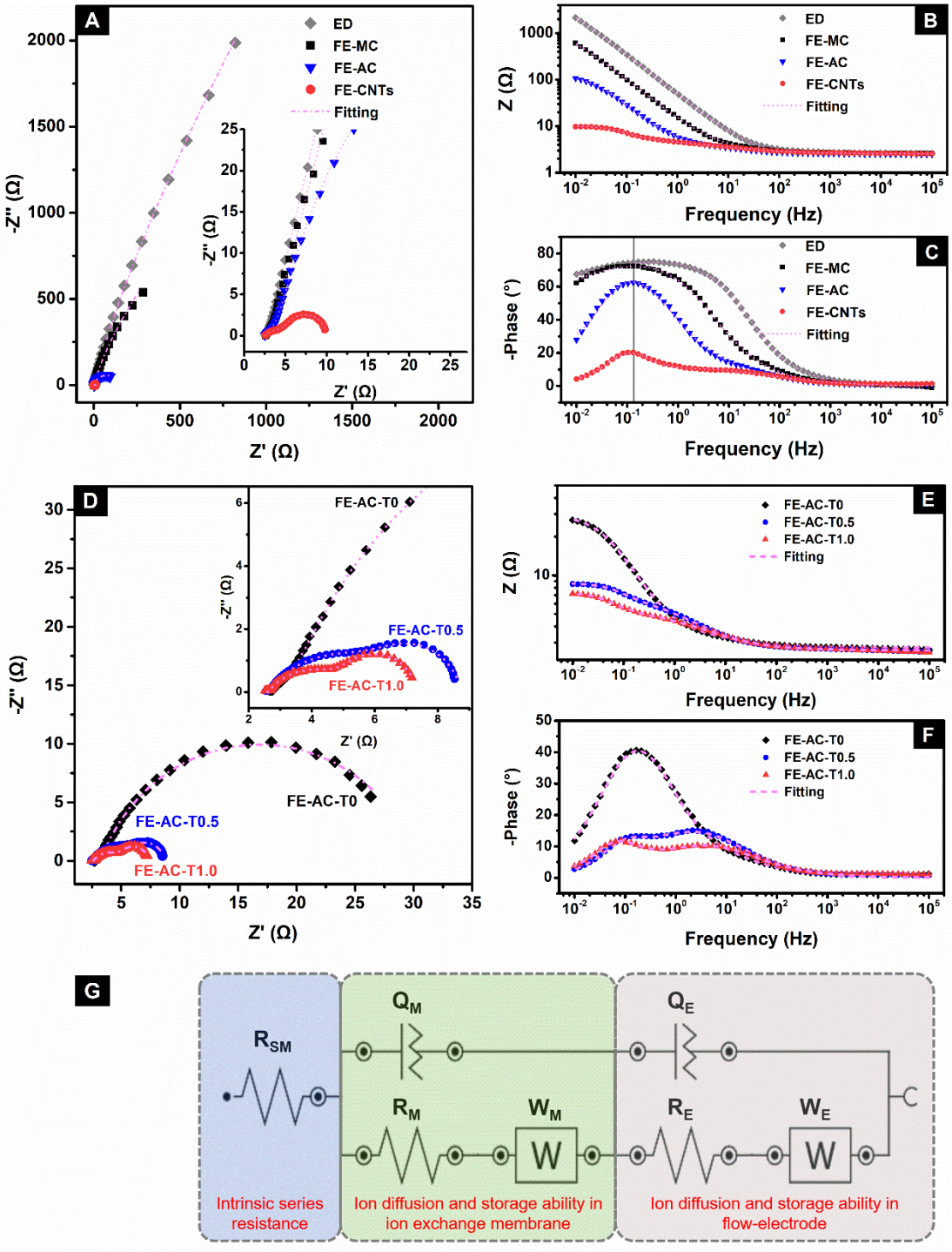

Figure 3 Electrochemical impedance spectroscopy (EIS) of flow-electrodes using different carbon powders at 3 wt.% carbon loading (A-C) and AC flow-electrodes using CNTs as additives with total carbon loading at 7.41 wt.% (D-E): Nyquist plots (A, D) and the corresponding bode modules (B, E) and phase diagrams (C, F). The simulated equivalent circuit for EIS signals is shown in (G).

Table 1 Fitting parameters obtained from simulated components of electrochemical impedance spectroscopy of flow-electrodes measured in flow mode

Flow-electrodes	R_{SM} (Ω)	Q_M Y0 (mMho)	Q_M N	R_M (Ω)	W_M (mMho)	Q_E Y0 (mMho)	Q_E N	R_E (Ω)	W_E (mMho)	x^2
ED	2.60	0.273	0.994	63.5	115	4.2	0.889	1627	0.656	0.0030
FE-MC	2.60	0.320	0.999	48.2	102	16.4	0.924	603	3.95	0.0200
FE-AC	2.50	30.5	0.697	1.36	286	63.0	0.956	99.3	333	0.0183
FE-CNTs	2.55	79.8	0.502	2.96	NA	478	0.990	4.56	NA	0.0049
FE-AC-T0	2.74	107	0.609	0.80	NA	103	0.815	26.6	NA	0.0180
FE-AC-T0.5	2.60	67.9	0.608	4.17	NA	995	1.000	2.01	NA	0.0073
FE-AC-T1.0	2.61	75.2	0.590	2.61	NA	1350	0.970	2.12	NA	0.0122

As shown in Figures 3A to 3C, FEs containing 3 wt.% carbon powders demonstrated completely different EIS responses. The real (Z') and imaginary (-Z'') resistance components in the Nyquist plot (Figure 3A), as well as the equivalent circuit resistance ($|Z| = |Z'| + |-Z''|$, Figure 3B) decreased significantly in the order of ED, MC, AC, and CNTs, suggesting enhanced electroconductivity of FE-CNTs. Furthermore, according to the phase change vs signal frequency (Figure 3C), FEs with enhanced electroconductivity in a running FCDI system, i.e. FE-CNTs, act more like a resistor with a low resistance rather than a capacitor because the phase lag in the low frequency region (close to a DC signal) is far less than 90 degrees. By contrast, a stationary porous carbon electrode generally acts as a capacitive component in the low frequency region because of a phase lag close to 90 degrees.[39-40] Moreover, FE-CNTs allows a high frequency signal to pass smoothly, suggesting a capacitive component with high frequency in the circuit as well. The combination of the phase changes in the high and low frequency regions indicates that FE-CNTs

are able to store more ions due to high capacitance and can enable fast charge transfer due its low series resistivity.

As shown in Figures 3D and 3E and Table 1, the conductivity of FEs can be further enhanced by increasing the carbon loading (3.7 times better for FE-AC-T0 at 7.41 wt.% vs FE-AC at 3 wt.%), as well as using CNTs as an additive (13.2 times better for FE-AC-T0.5 vs FE-AC-T0). Because of the enhanced electroconductivity, the current signal phase change in the region of medium to low frequency further decreased (Figure 3F). Note that, for the FEs showing phase hysteresis less than 20º in the low frequency region (Figures 3C and 3F), there were two peaks observed, indicating that there are two components (e.g., IEMs and FEs) affecting the EIS response.

Based on the results and discussion from Figures 3A to 3F, the FEs listed in Table 1 can fall into two categories, i.e., FEs with relatively poor (ED, FE-AC, FE-MC) or good (FE-AC-T0, FEs containing CNTs) electroconductivity.

To clearly understand the electrochemical behavior of FEs in a running FCDI system, we proposed an equivalent circuit (Figure 3G) to simulate the EIS signals (Figure 3A to 3F). The fitting parameters for this equivalent circuit are summarized in Table 1. As shown in Figure 3G, the electrochemical elements for the small FCDI device can be considered as three parts: (i) the series resistances of FS and IEMs and the contact resistance between phases (R_{SM}); (ii) the ion transport and diffusion from feed solution into IEMs (R_M, Q_M and W_M); (iii) the ion transport and diffusion from IEMs into FEs (R_E, Q_E and W_E). The Y0 and N values of Q_M and Q_E are related to the capacitance (C) according to the calculation $C = \mathrm{Y0}^{\left(\frac{1}{\mathrm{N}}\right)} \times \mathrm{R}^{\left(\frac{1}{\mathrm{N}} - 1\right)}$. It should be noted that the elements representing ion diffusion and transport in IEMs and FEs (Figure 3G) include the characteristics of anion and cation exchange membranes, and anode and cathode, as well.

The R_{SM} values for all FEs of the FCDI device were similar because the operating conditions and the membranes employed were identical. For FCDI systems using FEs with poor conductivity, the ions transport (R) and diffusion resistances (W) in IEMs (R_M, W_M) and FEs (R_E, W_E) were high, and the capacitive equivalent components (Q_M and Q_E) were low, suggesting that the IEMs and FEs likely acted as charge/ion resistors rather than conductors. For FEs with high conductivity, the equivalent circuit can be well-simulated only when the diffusion resistance (W_E & W_M) is negligible, which means ion-transport-mechanism dominated ion removal. FEs with high conductivity acted as ideal capacitors due to the extremely low R_E and high Q_E values (Table 1). In addition, because the values of the simulated parameter N of the constant phase elements for IEMs (Q_M) deviated from 1 to 0.5, while the N values of Q_E and Q_M were close to 1,[41] ion removal was primarily controlled by the ion exchange capacity of IEMs.

Overall, it is also worthy to note that the capacitance of FEs may keep increasing due to the subsequent discharging of FEs outside the flowing FCDI module; therefore, the low resistance of FEs is more critical in guiding the electrochemical performance of FEs. Furthermore, the analysis of the EIS results suggests that the electroconductivity of FEs is mainly governed by the intrinsic properties of carbon materials, and it can be further enhanced by increasing the carbon loading, as well as adding CNTs as additive.

The increased conductivity of FE-CNTs is also likely to reduce the overpotentials of Faradaic processes, thereby suppressing the Faradaic reactions of FE-CNTs, increasing the charge efficiency and ultimately improving the desalination performance. Generally, overpotentials of Faradaic processes would be generated when there is electrochemical polarization, or concentration polarization, or resistance polarization on the electrode-electrolyte interface.[42] These polarizations can be reduced by ensuring that charges are transported in the form of electrons in

the electrodes and ions in the solution, rather than Faraday reactions on the electrode-electrolyte interface. Correspondingly, there are three strategies to decrease the overpotentials: (i) increasing effective surface area to decrease the charge density on the electrodes;[43] (ii) increasing the ion diffusion rates in the carbon pores by controlling the pore structure (e.g., large pore size);[44] and (iii) increasing the electrode conductivity to reduce ohmic overpotential.[45]

With respect to the first strategy, compared to the ED process, the increased electrode area of the carbon flow-electrodes should be the reason for the suppressed Faradaic reactions. Compared to MC and AC, however, CNTs had the lowest surface area (Table S5) and FE-CNTs demonstrated the best desalination performance. Thus, the increased surface area should not be the reason for the decreased overpotentials of Faradaic processes for FE-CNTs. For the second strategy, as shown in Table S5, the average pore widths of the three carbon powders were in the range of mesopores, which are much larger than the diameters of hydrated sodium and chloride ions (< 0.8 nm). In addition, in the FCDI devices using carbon flow-electrodes, the concentration differences between electrolyte and feed solutions were the same. These results indicate that the concentration polarization behavior was similar in all carbon flow-electrode cases. For the third strategy, according to the EIS results (Table 1), after the addition of carbon powders in the electrolyte, the R_E values of flow-electrodes was significantly reduced. Therefore, the main reason for the reduced overpotentials of Faradaic processes is the increased electroconductivity of the electrodes, as only the electroconductivity is positively correlated with the desalination performance of flow-electrodes.

Enhanced charge/ion transfer in FEs containing CNTs. Based on FCDI desalination performance and EIS analysis, we confirmed that the key factor for ensuring rapid FCDI desalination was the use of high-conductivity FEs. When using CNTs as a conductive additive to

FE-AC-T0, however, the addition of 0.5 wt.% was as effective as that of 1.0 wt.%, even though the electroconductivity of the latter was higher. This is because, when the conductivity increases beyond a certain value, another factor involved in ion removal may become the limiting mechanism. Possible candidates that can limit the process include: diffusion through IEMs and diffusion through the electrolyte solution. The latter becomes important when the viscosity increases, which happens as more CNTs are added to the carbon suspension (Figure 4A).

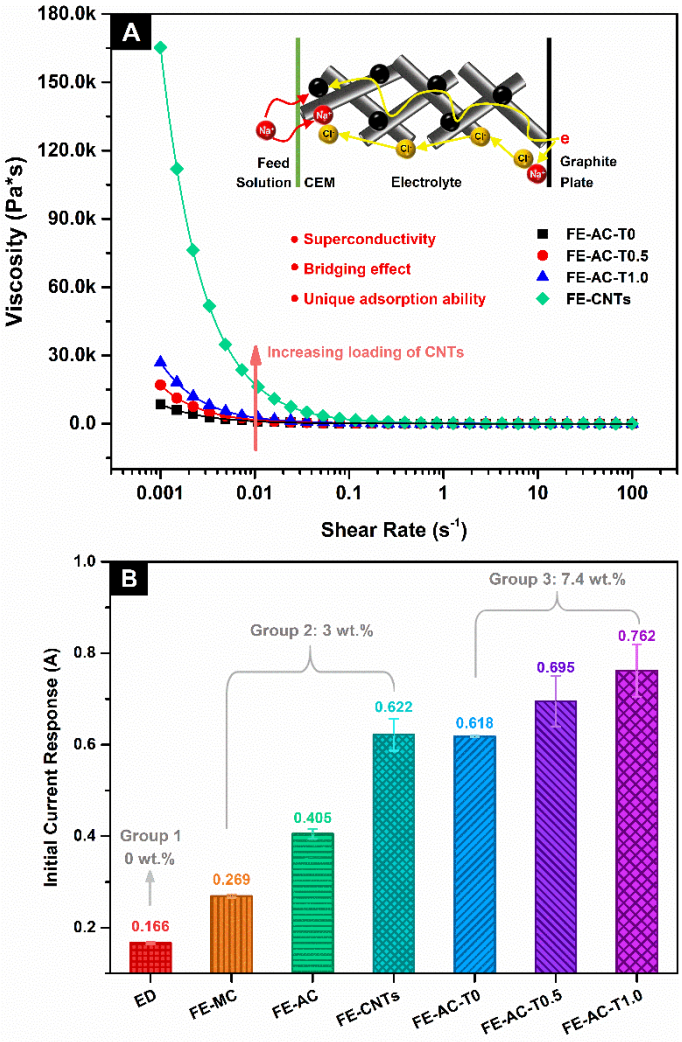

Figure 4 (A) Rheological properties of flow-electrodes containing carbon nanotubes (CNTs), where the shear rate decreases from 100 to 0.001 s^{-1}. (B) Initial current response in FCDI systems using flow-electrodes of different carbon content.

Table S7 shows the rheological parameters of FEs containing CNTs, where the simulated consistency index k is related to the fluid viscosity through eq. S4.[12] The limiting behavior of high-viscosity FE is flow clogging. The viscosity increase of FE-AC-T0.5 is relatively small compared to that of the FE-AC-T0, but its conductivity is increased by 1323%. The viscosity of FE-AC-T1.0, however, almost doubled, while the conductivity is similar to that of FE-AC-T0.5. From the experimental data of Table S6, the salt removal ability of FE-CNTs was intrinsically much greater than that of other FEs. It is interesting to note here that the *SRC* value for the 3 wt.% CNTs in FE was 284.3 mg g^{-1} carbon, while for 7.41 wt.% AC in FE, the *SRC* value was 121.7 mg g^{-1} carbon. This difference corresponds to 234% greater *SRC* for FE-CNTs at 3 wt.% than for the second-best carbon at 7.41 wt.% (FE-AC-T0), while the electroconductivity of FE-CNTs is increased by 583% and its viscosity by 1298%. These results indicate that high electroconductivity is needed for enhanced ion-removal rates. It is also important to note that high viscosity may cause problems with increased pump energy consumption and blockage of the FE channels.

According to the FE composition used in this study, FEs can be classified into three types, (i) carbon-free FE (ED), (ii) FE using carbon particles having a random shape, e.g., AC and MC, and (iii) FE containing CNTs. Accordingly, three kinds of charge/ion migration paths for these three types of FEs are proposed here (Figure 5):

(i) Carbon-free FE (Electrodialysis system): Electrolyte is the only charge/ion transfer medium in a carbon-free FE with water as the main content. Since water has high resistance, the charge/ion transfer in a carbon-free FE relies on the number of ions in the electrolyte.

(ii) FEs using carbon particles with random size and shape: In addition to the paths in electrolyte, charge/ion transfer could occur by collisions among carbon particles and between carbon particles and current collector.[16]

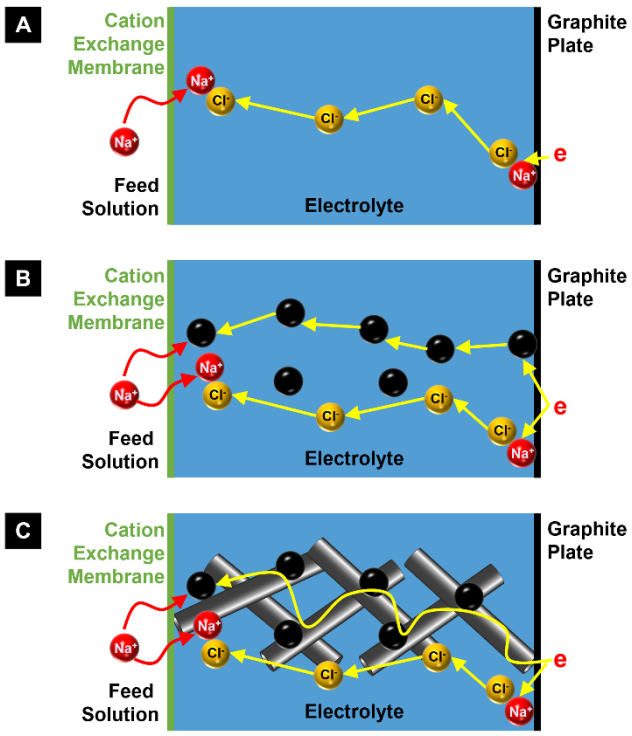

Figure 5 Proposed ion and charge transfer mechanism inside (A) electrodialysis system, (B) FCDI system using regular carbon powders, and (C) FCDI system using CNTs.

(iii) FEs using CNTs as additive for carbon particles: Except for the two routes described above, charge can be easier transferred based on the bridging effect of conductive nanotubes. Since CNTs are a kind of tubular elongated carbon material compared to granular carbon particles, the hypothesis is that CNTs are more likely to collide with each other and keep in contact with each other during flow.

To further examine the proposed hypothesis, we plotted the initial current responses of the above three types of FEs in Figure 4B. The current generated by the electrolyte is 0.166 A; after loading the regular carbon particles (MC and AC), the current of the FEs is increased to 0.269 and 0.405 A, respectively, which is 1.6 to 2.4 times better that of the electrolyte alone; with the same amount of CNTs (3 wt.%) added, FE-CNTs have a current response of 0.622 A, which is comparable to an AC based FE with a load of 7.41 wt% (0.618 A). When CNTs are used as additive for FE-

AC-T0, the current response shows a linear relationship with the amount of CNTs added (0, 0.5 and 1 wt.%). Quantitatively, the current increased by 12.5% and 9.6%, respectively, as the CNTs content was increased from 0 to 0.5 to 1.0 wt.%. As the current is proportional to the electroconductivity, these results confirm that CNTs can increase the electroconductivity of FEs. The slope of increase, however, is much lower than the values reported on Table 1. The difference is that current measurements reveal the overall conductivity of the system, while the conductivity values of Table 1 are specifically for the FEs. This discrepancy reveals that, as the conductivity of the FEs increases, other transport processes in the system may become the limiting mechanism to ion/charge transfer.

For a low-cost, continuous, and energy-efficient FCDI system, carbon materials in the FE should have the following characteristics for high and fast salt removal: first, they should be inexpensive to maintain a low material cost for long-term operation; second, they should have high porosity to avoid particle settling and aggregation, while providing enough ion storage area; third, collisions among particles of the carbon material or between particles and current collectors should be maintained at high frequency; forth and most important, the FE conductivity must be high enough to ensure that charge/ion migration can proceed directly through interconnected carbon materials. As shown in Table S8, for flow-electrodes with *ASRR* values greater than 10 mg s^{-1} m^{-2}, they either had a high carbon loading (more than 20 wt.%)[13, 16] or the concentration of feed solution was significantly higher than the electrolyte concentration (increased driving force for ion transfer).[11] In our case, even with a low carbon loading (3 or 7.4 wt.%) and the same concentration of feed and electrolyte solutions (0.2 M), the FE-CNTs and FE-AC-T0.5 still demonstrated relatively high *ASRR* values. Note that the *ASRR* values in this work were based on twice the contact area between flow-electrodes and feed solution since both anion and cation exchange membranes were used

when one salt molecule was removed. This comparative study further indicates that, when using CNTs as an additive of AC-based FEs, the material cost can be significantly reduced since a much lower carbon loading is needed to achieve a relatively high desalination rate.

CONCLUSIONS

Based on the morphology and structure characterization, electrochemical testing, and application in FCDI, we found that CNTs achieved the highest (284.3 mg g^{-1} in 6 hours) and fastest (8.32 mg s^{-1} m^{-2}) salt removal for an initial FS concentration of 0.2 M NaCl, which is a result of the adsorption behavior of CNTs, their high electroconductivity and the enhancement in conductivity contributed by the bridging effect of CNTs. CNTs could increase the desalination rate of FE-AC-T0 by 34% at an optimized addition of 0.5 wt.%, due to the significant improvement in the electroconductivity (13.2 times better for FE-AC-T0.5 vs FE-AC-T0) with only slight increase in viscosity, resulting in a salt removal efficiency of 93.6% and an average salt removal rate of 13.16 mg s^{-1} m^{-2}. The high electroconductivity of CNTs-contained FEs was confirmed by EIS analysis. Compared to the capacitance and viscosity, electroconductivity is more critical in determining the FCDI performance than the flowing characteristics of FEs. A path was proposed for the transfer of charge/ion in CNTs-containing FEs, i.e., (i) transport of ions through the electrolyte, (2) transport through collisions between particles, and (3) transport through bridged CNTs, which is the fastest path. As these same mechanisms occur during regeneration of the anion and cation loaded carbon particles at the exit of the FCDI cell, addition of CNTs should be expected to accelerate regeneration as well. Finally, according to the bridging effect provided by the CNTs, other relatively inexpensive carbon materials having tubular, planar, or fiber structures, including graphene and carbon fibers, should be investigated for their FCDI desalination performance. The

results of this study are also applicable to energy storage devices, including ultracapacitors and batteries, which are important for energy sustainability.

ASSOCIATED CONTENT

Supporting Information

Supporting information for this article is available free of charge on the ACS Publications website. Materials, properties of ion exchange membranes and graphite current collectors, calculation methods, schematic of the FCDI process, the composition of flow-electrodes, characterization method, results and discussion about the morphology and structure of carbon materials, tables of desalination performance using various FEs, rheological properties of FEs and abbreviations used in the manuscript are included in the Supporting Information.

AUTHOR INFORMATION

Corresponding Authors

*Tel.: +1 865 241 3246; e-mail: tsourisc@ornl.gov

Notes

The authors declare no competing financial interest.

ACKNOWLEDGMENTS

Notice: This manuscript has been authored by UT-Battelle, LLC under Contract No. DE-AC05-00OR22725 with the US Department of Energy. The United States Government retains and the publisher, by accepting the article for publication, acknowledges that the United States Government retains a non-exclusive, paid-up, irrevocable, world-wide license to publish or reproduce the published form of this manuscript, or allow others to do so, for United States Government purposes. The Department of Energy will provide public access to these results of

federally sponsored research in accordance with the DOE Public Access Plan (http://energy.gov/downloads/doe-public-access-plan).

The authors would like to thank the School of Civil and Environmental Engineering of the Georgia Institute of Technology and the National Natural Science Foundation of China (NSFC) for financial support via Grant numbers 51425405 and 21377130. Kexin Tang appreciates financial support from China Scholarship Council (CSC, No. 201606250079). Costas Tsouris acknowledges support from the Laboratory Directed Research and Development Program of the Oak Ridge National Laboratory. The authors thank Alexander Wiechert for editing the manuscript.

REFERENCES

(1) Suss, M. E.; Porada, S.; Sun, X.; Biesheuvel, P. M.; Yoon, J.; Presser, V. Water desalination via capacitive deionization: what is it and what can we expect from it? *Energ. Environ. Sci.* **2015,** *8* (8), 2296-2319, DOI 10.1039/c5ee00519a.

(2) Biesheuvel, P. M.; van der Wal, A. Membrane capacitive deionization. *J. Membr. Sci.* **2010,** *346* (2), 256-262, DOI 10.1016/j.memsci.2009.09.043.

(3) Chang, J. J.; Tang, K. X.; Cao, H. B.; Zhao, Z. J.; Su, C. L.; Li, Y. P.; Duan, F.; Sheng, Y. X. Application of anion exchange membrane and the effect of its properties on asymmetric membrane capacitive deionization. *Sep. Purif. Technol.* **2018,** *207*, 387-395, DOI 10.1016/j.seppur.2018.06.063.

(4) Huang, Z. H.; Yang, Z. Y.; Kang, F. Y.; Inagaki, M. Carbon electrodes for capacitive deionization. *J. Mater. Chem. A* **2017,** *5* (2), 470-496, DOI 10.1039/c6ta06733f.

(5) Suss, M. E.; Baumann, T. F.; Bourcier, W. L.; Spadaccini, C. M.; Rose, K. A.; Santiago, J. G.; Stadermann, M. Capacitive desalination with flow-through electrodes. *Energ. Environ. Sci.* **2012,** *5* (11), 9511-9519, DOI 10.1039/c2ee21498a.

(6) Bian, Y. H.; Liang, P.; Yang, X. F.; Jiang, Y.; Zhang, C. Y.; Huang, X. Using activated carbon fiber separators to enhance the desalination rate of membrane capacitive deionization. *Desalination* **2016,** *381*, 95-99, DOI 10.1016/j.desal.2015.11.016.

(7) Garcia-Quismondo, E.; Santos, C.; Lado, J.; Palma, J.; Anderson, M. A. Optimizing the energy efficiency of capacitive deionization reactors working under real-world conditions. *Environ. Sci. Technol.* **2013,** *47* (20), 11866-11872, DOI 10.1021/es4021603.

(8) Lu, D.; Cai, W. F.; Wang, Y. Optimization of the voltage window for long-term capacitive deionization stability. *Desalination* **2017,** *424*, 53-61, DOI 10.1016/j.desal.2017.09.026.

(9) Wenten, I. G.; Khoiruddin, K.; Aryanti, P. T. P.; Hakim, A. N. Scale-up Strategies for Membrane-Based Desalination Processes: A Review. *J. Membr. Sci. Res.* **2016,** *2* (2), 42-58, DOI 10.22079/jmsr.2016.19152.

(10) Park, B. H.; Choi, J. H. Improvement in the capacitance of a carbon electrode prepared using water-soluble polymer binder for a capacitive deionization application. *Electrochim. Acta* **2010,** *55* (8), 2888-2893, DOI 10.1016/j.electacta.2009.12.084.

(11) Jeon, S. I.; Park, H. R.; Yeo, J. G.; Yang, S.; Cho, C. H.; Han, M. H.; Kim, D. K. Desalination via a new membrane capacitive deionization process utilizing flow-electrodes. *Energ. Environ. Sci.* **2013,** *6* (5), 1471-1475, DOI 10.1039/c3ee24443a.

(12) Hatzell, K. B.; Hatzell, M. C.; Cook, K. M.; Boota, M.; Housel, G. M.; McBride, A.; Kumbur, E. C.; Gogotsi, Y. Effect of oxidation of carbon material on suspension electrodes for flow electrode capacitive deionization. *Environ. Sci. Technol.* **2015,** *49* (5), 3040-3047, DOI 10.1021/es5055989.

(13) Doornbusch, G. J.; Dykstra, J. E.; Biesheuvel, P. M.; Suss, M. E. Fluidized bed electrodes with high carbon loading for water desalination by capacitive deionization. *J. Mater. Chem. A* **2016,** *4* (10), 3642-3647, DOI 10.1039/c5ta10316a.

(14) Xu, X.; Wang, M.; Liu, Y.; Lu, T.; Pan, L. Ultrahigh Desalinization Performance of Asymmetric Flow-Electrode Capacitive Deionization Device with an Improved Operation Voltage of 1.8 V. *ACS Sustain. Chem. Eng.* **2016,** *5* (1), 189-195, DOI 10.1021/acssuschemeng.6b01212.

(15) Nativ, P.; Badash, Y.; Gendel, Y. New insights into the mechanism of flow-electrode capacitive deionization. *Electrochem. Commun.* **2017,** *76*, 24-28, DOI 10.1016/j.elecom.2017.01.008.

(16) Liang, P.; Sun, X. L.; Bian, Y. H.; Zhang, H. L.; Yang, X. F.; Jiang, Y.; Liu, P. P.; Huang, X. Optimized desalination performance of high voltage flow-electrode capacitive deionization by adding carbon black in flow-electrode. *Desalination* **2017,** *420*, 63-69, DOI 10.1016/j.desal.2017.05.023.

(17) Yang, S.; Choi, J.; Yeo, J. G.; Jeon, S. I.; Park, H. R.; Kim, D. K. Flow-Electrode Capacitive Deionization Using an Aqueous Electrolyte with a High Salt Concentration. *Environ. Sci. Technol.* **2016,** *50* (11), 5892-5899, DOI 10.1021/acs.est.5b04640.

(18) Park, H. R.; Choi, J.; Yang, S.; Kwak, S. J.; Jeon, S. I.; Han, M. H.; Kim, D. K. Surface-modified spherical activated carbon for high carbon loading and its desalting performance in flow-electrode capacitive deionization. *RSC Adv.* **2016,** *6* (74), 69720-69727, DOI 10.1039/c6ra02480g.

(19) Ma, J.; He, D.; Tang, W.; Kovalsky, P.; He, C.; Zhang, C.; Waite, T. D. Development of Redox-Active Flow Electrodes for High-Performance Capacitive Deionization. *Environ. Sci. Technol.* **2016,** *50* (24), 13495-13501, DOI 10.1021/acs.est.6b03424.

(20) Akuzum, B.; Agartan, L.; Locco, J.; Kumbur, E. C. Effects of particle dispersion and slurry preparation protocol on electrochemical performance of capacitive flowable electrodes. *J. Appl. Electrochem.* **2017,** *47* (3), 369-380, DOI 10.1007/s10800-017-1046-5.

(21) Chen, J.; Hamon, M. A.; Hu, H.; Chen, Y.; Rao, A. M.; Eklund, P. C.; Haddon, R. C. Solution properties of single-walled carbon nanotubes. *Science* **1998,** *282* (5386), 95-98, DOI 10.1126/science.282.5386.95.

(22) Kaempgen, M.; Chan, C. K.; Ma, J.; Cui, Y.; Gruner, G. Printable thin film supercapacitors using single-walled carbon nanotubes. *Nano Lett.* **2009,** *9* (5), 1872-1876, DOI 10.1021/nl8038579.

(23) Izadi-Najafabadi, A.; Yasuda, S.; Kobashi, K.; Yamada, T.; Futaba, D. N.; Hatori, H.; Yumura, M.; Iijima, S.; Hata, K. Extracting the full potential of single-walled carbon nanotubes as durable supercapacitor electrodes operable at 4 V with high power and energy density. *Adv. Mater.* **2010,** *22* (35), E235-E241, DOI 10.1002/adma.200904349.

(24) Dang, X.; Yi, H.; Ham, M. H.; Qi, J.; Yun, D. S.; Ladewski, R.; Strano, M. S.; Hammond, P. T.; Belcher, A. M. Virus-templated self-assembled single-walled carbon nanotubes for highly efficient electron collection in photovoltaic devices. *Nat. Nanaotechnol.* **2011,** *6* (6), 377-384, DOI 10.1038/nnano.2011.50.

(25) Rajalakshmi, N.; Dhathathreyan, K. S.; Govindaraj, A.; Satishkumar, B. C. Electrochemical investigation of single-walled carbon nanotubes for hydrogen storage. *Electrochim. Acta* **2000,** *45* (27), 4511-4515, DOI 10.1016/S0013-4686(00)00510-7.

(26) Zhou, G.; Duan, W.; Gu, B. Electronic structure and field-emission characteristics of open-ended single-walled carbon nanotubes. *Phys. Rev. Lett.* **2001,** *87* (9), 095504, DOI 10.1103/PhysRevLett.87.095504.

(27) Cao, Q.; Rogers, J. A. Ultrathin Films of Single-Walled Carbon Nanotubes for Electronics and Sensors: A Review of Fundamental and Applied Aspects. *Adv. Mater.* **2009,** *21* (1), 29-53, DOI 10.1002/adma.200801995.

(28) Futaba, D. N.; Hata, K.; Yamada, T.; Hiraoka, T.; Hayamizu, Y.; Kakudate, Y.; Tanaike, O.; Hatori, H.; Yumura, M.; Iijima, S. Shape-engineerable and highly densely packed single-walled carbon nanotubes and their application as super-capacitor electrodes. *Nat. Mater.* **2006,** *5* (12), 987-994, DOI 10.1038/nmat1782.

(29) Lee, B.; Park, N.; Kang, K. S.; Ryu, H. J.; Hong, S. H. Enhanced Capacitive Deionization by Dispersion of CNTs in Activated Carbon Electrode. *ACS Sustain. Chem. Eng.* **2018,** *6* (2), 1572-1579, DOI 10.1021/acssuschemeng.7b01750.

(30) Ajayan, P. M.; Schadler, L. S.; Giannaris, C.; Rubio, A. Single-walled carbon nanotube-polymer composites: Strength and weakness. *Adv. Mater.* **2000,** *12* (10), 750-753, DOI 10.1002/(Sici)1521-4095(200005)12:10<750::Aid-Adma750>3.0.Co;2-6.

(31) Li, H. B.; Pan, L. K.; Lu, T.; Zhan, Y. K.; Nie, C. Y.; Sun, Z. A comparative study on electrosorptive behavior of carbon nanotubes and graphene for capacitive deionization. *J. Electroanal. Chem.* **2011,** *653* (1-2), 40-44, DOI 10.1016/j.jelechem.2011.01.012.

(32) Moronshing, M.; Subramaniam, C. Scalable Approach to Highly Efficient and Rapid Capacitive Deionization with CNT-Thread As Electrodes. *ACS Appl. Mater. Inter.* **2017,** *9* (46), 39907-39915, DOI 10.1021/acsami.7b11866.

(33) Krupke, R.; Hennrich, F.; Lohneysen, H.; Kappes, M. M. Separation of metallic from semiconducting single-walled carbon nanotubes. *Science* **2003,** *301* (5631), 344-347, DOI 10.1126/science.1086534.

(34) Choo, K. Y.; Yoo, C. Y.; Han, M. H.; Kim, D. K. Electrochemical analysis of slurry electrodes for flow-electrode capacitive deionization. *J. Electroanal. Chem.* **2017,** *806*, 50-60, DOI 10.1016/j.jelechem.2017.10.040.

(35) Hatzell, K. B.; Iwama, E.; Ferris, A.; Daffos, B.; Urita, K.; Tzedakis, T.; Chauvet, F.; Taberna, P. L.; Gogotsi, Y.; Simon, P. Capacitive deionization concept based on suspension electrodes without ion exchange membranes. *Electrochem. Commun.* **2014,** *43*, 18-21, DOI 10.1016/j.elecom.2014.03.003.

(36) Długołęcki, P.; Anet, B.; Metz, S. J.; Nijmeijer, K.; Wessling, M. Transport limitations in ion exchange membranes at low salt concentrations. *J. Membr. Sci.* **2010,** *346* (1), 163-171, DOI 10.1016/j.memsci.2009.09.033.

(37) Guo, R. Q.; Wang, B. B.; Jia, Y. X.; Wang, M. Development of acid block anion exchange membrane by structure design and its possible application in waste acid recovery. *Sep. Purif. Technol.* **2017,** *186*, 188-196, DOI 10.1016/j.seppur.2017.06.006.

(38) Ma, J.; He, C.; He, D.; Zhang, C.; Waite, T. D. Analysis of capacitive and electrodialytic contributions to water desalination by flow-electrode CDI. *Water Res.* **2018,** *144*, 296-303, DOI 10.1016/j.watres.2018.07.049.

(39) Tang, K. X.; Chang, J. J.; Cao, H. B.; Su, C. L.; Li, Y. P.; Zhang, Z. S.; Zhang, Y. Macropore- and Micropore-Dominated Carbon Derived from Poly(vinyl alcohol) and Polyvinylpyrrolidone for Supercapacitor and Capacitive Deionization. *ACS Sustain. Chem. Eng.* **2017,** *5* (12), 11324-11333, DOI 10.1021/acssuschemeng.7b02307.

(40) Tang, K. X.; Li, Y. P.; Li, Y. J.; Cao, H. B.; Zhang, Z. S.; Zhang, Y.; Yang, J. Self-reduced VO/VOx/carbon nanofiber composite as binder-free electrode for supercapacitors. *Electrochim. Acta* **2016,** *209*, 709-718, DOI 10.1016/j.electacta.2016.05.051.

(41) Kochowski, S.; Nitsch, K. Description of the frequency behaviour of metal–SiO2–GaAs structure characteristics by electrical equivalent circuit with constant phase element. *Thin Solid Films* **2002,** *415* (1-2), 133-137, DOI 10.1016/s0040-6090(02)00506-0.

(42) Bard, A. J.; Faulkner, L. R. *Electrochemical methods: fundamentals and applications*, New York: Wiley, c2001. 2nd ed.: 2001.

(43) Kim, S.; Koratkar, N.; Karabacak, T.; Lu, T.-M. Water electrolysis activated by Ru nanorod array electrodes. *Appl. Phys. Lett.* **2006,** *88* (26), 263106, DOI 10.1063/1.2218042.

(44) Sun, B.; Huang, X.; Chen, S.; Munroe, P.; Wang, G. Porous Graphene Nanoarchitectures: An Efficient Catalyst for Low Charge-Overpotential, Long Life, and High Capacity Lithium–Oxygen Batteries. *Nano Lett.* **2014,** *14* (6), 3145-3152, DOI 10.1021/nl500397y.

(45) Zeng, K.; Zhang, D. Recent progress in alkaline water electrolysis for hydrogen production and applications. *Prog. Energy Combust. Sci.* **2010,** *36* (3), 307-326, DOI 10.1016/j.pecs.2009.11.002.

Graphical Abstract

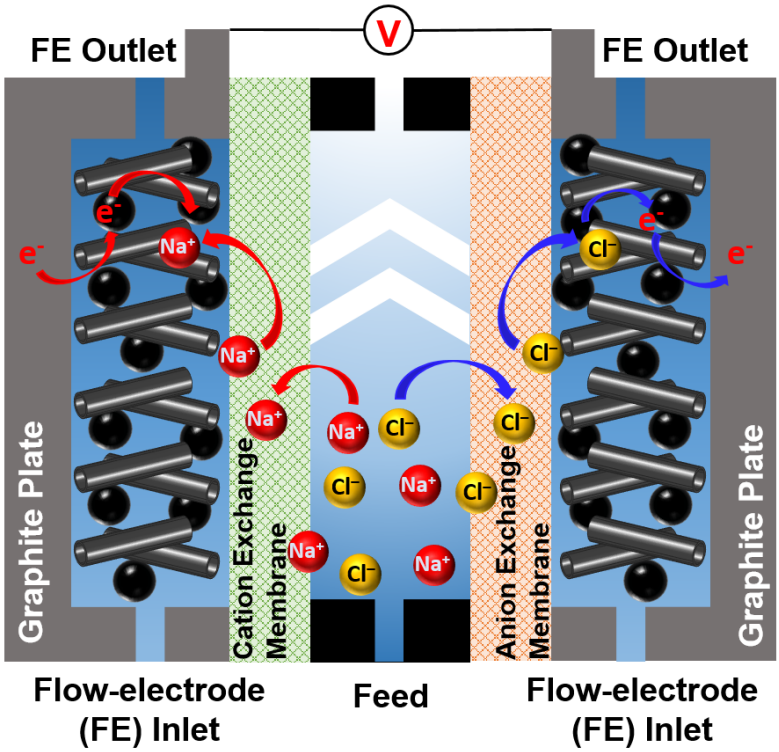

Synopsis: Flow electrodes containing carbon nanotubes exhibit excellent charge efficiency toward a sustainable desalination process.